Effect of Ammonia or Nitric Acid Treatment on Surface Structure, *in vitro* Apatite Formation, and Visible-Light Photocatalytic Activity of Bioactive Titanium Metal

Masakazu Kawashita[a,*], Naoko Matsui[a], Toshiki Miyazaki[b], Hiroyasu Kanetaka[c]

[a]*Graduate School of Biomedical Engineering, Tohoku University, Sendai 980-8579, Japan*

[b]*Graduate School of Life Science and Systems Engineering, Kyushu Institute of Technology, Kitakyushu 808-0196, Japan*

[c]*Liaison Center for Innovative Dentistry, Graduate School of Dentistry, Tohoku University, Sendai 980-8575, Japan*

*Corresponding author

Tel.: +81-22-795-3937; Fax: +81-22-795-4735

E-mail: m-kawa@ecei.tohoku.ac.jp

Abstract

Ti metal treated with NaOH, NH_4OH, and heat and then soaked in simulated body fluid (SBF) showed *in vitro* apatite formation whereas that treated with NaOH, HNO_3, and heat and then soaked in SBF did not. The anatase TiO_2 precipitate and/or the fine network structure formed on the surface of the Ti metal treated with NaOH, NH_4OH, and heat and then soaked in SBF might be responsible for the formation of apatite on the surface of the metal. The NaOH, NH_4OH, and heat treatments might produce nitrogen-doped TiO_2 on the surface of the Ti metal, and the concentration of methylene blue (MB) in the Ti metal sample treated with NaOH, NH_4OH, and heat decreased more than in the untreated and NaOH- and heat-treated ones. This preliminary result suggests that Ti metal treated with NaOH, NH_4OH, and heat has the potential to show photocatalytic activity under visible light.

Keywords: titanium metal; titania; nitrogen; apatite; visible-light photocatalytic activity; simulated body fluid

1. Introduction

Postoperative infection is a serious problem that occurs because of the growth of bacteria on the surface of metallic orthopedic implants. Although the incidence of surgical site infection (SSI) depends on the surgical sites themselves and on the operative procedures, it has previously been reported that the incidence of SSI for artificial hip joints was 0.2–0.6% [1-3] and for artificial knee joints was 2.2–2.9% [2, 4, 5]. When implants were externally fixed, the incidence of SSI was 51% [6]. Unfortunately when infection occurs, a surgical operation is essential to replace the implants at worst, resulting in a remarkable decrease in quality of life (QOL) for patients. Therefore, it is desirable to develop antibacterial, biocompatible metallic implants in order to minimize the incidence of SSI and thus minimize the need for implant replacement.

Numerous attempts have been made to develop antibacterial, biocompatible metallic implants including silver-coated [7, 8] and silver-containing-hydroxyapatite-coated metallic implants [9, 10]; however, silver is toxic to human cells [11, 12]. Silver-free antibacterial metallic implants and iodine-supported titanium implants were recently developed [13], and good clinical results have been reported [14].

About 15 years ago, treating titanium (Ti) metal and its alloys with sodium hydroxide (NaOH) and subsequently heating them [15] was found to induce bone bonding (*i.e.*, bioactivity) on implants produced from them [16]. A NaOH- and heat-treated artificial hip joint produced from Ti-6Al-2Nb-Ta alloy was clinically used in Japan for the first time in 2007 [17]. However, because NaOH- and heat-treated Ti metal does not exhibit antibacterial properties, silver-doped bioactive Ti metal has recently been used as a material for implants [18] despite concerns about the cytotoxicity of silver.

It has previously been reported that sodium titanate and titania (TiO_2) containing rutile and anatase structures, which are formed on the surface of NaOH- and heat-treated Ti metal and its alloys, are responsible for the bioactivity [15]. Further, the TiO_2 layer that forms on Ti metal during anodic oxidation shows *in vitro* apatite formation [19, 20] and *in vivo* bone bonding [21]. It has previously been reported that nitrogen (N)-doped TiO_2, on the other hand, shows visible-light-induced photocatalytic activity [22-24]. Therefore, if N atoms are successfully incorporated into the surface TiO_2 layer on Ti metal to induce photocatalytic activity with visible light, the resultant Ti metal would show not only *in vivo* bioactivity but also *ex-vivo* visible-light-induced antibacterial properties such as those induced under shadowless light in an operation room. It is expected that either aqueous ammonia (NH_4OH) or nitric acid (HNO_3) could be used to introduce N atoms into the surface of NaOH-treated Ti metal because the sodium-hydrogen-titanate-gel layer formed during NaOH treatment of Ti

metal would be highly reactive. In this study, we investigated apatite formation and visible-light photocatalytic activity of Ti metal subjected to a series of treatments: NaOH, either aqueous ammonia (NH_4OH) or nitric acid (HNO_3), and heat. The results are discussed in terms of the structures on the surface of the treated Ti metal.

2. Materials and Methods

2.1. Sample preparation

Commercially available pure Ti plates (10 mm × 10 mm × 1 mm; purity: 99.9%; Kojundo Chemical Laboratory, Japan) were used. They were abraded using No. 400 abrasive paper and then washed with pure acetone and ultrapure water in an ultrasonic cleaner. The Ti plates were soaked in 5 mL of 5 M NaOH solution at 60°C. The samples were subsequently soaked in 7 mL of either 1 M NH_4OH or 1 M HNO_3 at 40°C for 24 h and were then gently washed with ultrapure water and dried. Special grade NaOH (Wako Pure Chemical Industries, Japan), 28% NH_4OH (Wako Pure Chemical Industries, Japan), and HNO_3 (Wako Pure Chemical Industries, Japan) were used in this study. The samples were heated to 600°C at a rate of 5°C·min^{-1} in an electric furnace (MSFS-1218, Yamada Denki, Japan), maintained at this temperature for 1 h, and then naturally cooled to room temperature in the furnace. The abbreviated names of the samples subjected to various treatments are listed in Table 1.

2.2. Immersion of samples in simulated body fluid

The samples were soaked in 30 mL of simulated body fluid (SBF) [25, 26] containing ion concentrations (Na^+: 142.0 mM; K^+: 5.0 mM; Ca^{2+}: 2.5 mM; Mg^{2+}: 1.5 mM; Cl^-: 147.8 mM; HCO_3^-: 4.2 mM; HPO_4^{2-}: 1.0 mM; SO_4^{2-}: 0.5 mM) that were nearly identical to those in human blood plasma at 36.5°C, according to the ISO 23317: 2007 standard. After the samples had been immersed in SBF for 7 d, they were removed and gently washed with ultrapure water.

2.3. Characterization of sample surfaces

The surface structures of the samples were investigated using a thin-film X-ray diffractometer (TF-XRD; RINT-2200VL, Rigaku, Japan), scanning electron microscope (SEM; VE-8800, Keyence, Japan), and an X-ray photoelectron spectrometer (XPS; AXIS Ultra DLD, Kratos Analytical, U.K.). We used the following settings during the TF-XRD measurements. X-ray source: Ni-filtered Cu Kα radiation; X-ray power: 40 kV, 40 mA;

scanning rate: 2° min^{-1}; sampling angle: 0.02°. We used the following settings during the XPS measurements. X-ray source: monochromatic Al Kα radiation (1486.7 eV); X-ray power: 15 kV, 10 mA. The binding energy was calibrated using the C_{1s} photoelectron peak at 284.8eV as a reference. The XPS peak analysis was performed using CasaXPS Version 2.3.15 software with all spectra Shirley background subtracted prior to fitting. The elemental composition was calculated from XPS spectra using the specific relative sensitivity factors for the Kratos Axis Ultra (O_{1s}: 0.78, Ti_{2p}: 2.001, N_{1s}: 0.477, C_{1s}: 0.278).

2.4. Evaluation of visible-light photocatalytic activity

The visible-light photocatalytic activity of the samples was evaluated by examining the decomposition of methylene blue (MB; Waldeck, Germany), which is often used as a model substance. The samples were soaked in 5 mL of 0.01 mM MB aqueous solution and incubated for 24 h to reach adsorption equilibrium. The MB aqueous solution was then replenished, and the samples were irradiated with 400–700-nm wavelength fluorescent light (FPL27EX-N, Panasonic, Japan) for 6 h. The distance between the fluorescent light and the samples was fixed at 10 cm. Here, it is noted that the wavelength of the fluorescent light (400-700 nm) should be similar to that of light source in operation room, but the distance between fluorescent light and samples (10 cm) is not possible in operation room. However, in the present study, we aimed to investigate visible-light photocatalytic activity of samples fundamentally. Fundamental findings on the visible-light photocatalytic activity of samples can be obtained even in the present experimental condition. In future study, we should carry out the experiment under the real condition in operation room. The MB concentration in the irradiated samples was examined using an ultraviolet visual (UV-VIS) spectrophotometer (Sefi IUV-1240, As One, Japan) by measuring the UV absorbance at 664 nm. A schematic illustration of the apparatus is shown in Figure 1. The MB concentration was also measured in unsoaked samples as a control. The decrease in MB concentration (%) was calculated based on the difference in the concentration of MB in the soaked and unsoaked samples, C_{sample} and C_{blank}, respectively, as follows [27]:

$$\text{Decrease in concentration (\%)} = (C_{blank} - C_{sample}) \times 100/C_{blank} \quad (1)$$

3. Results and Discussion

Figure 2(a) shows SEM photographs of samples of Ti metal subjected to various surface treatments. A fine network structure had formed on the surface of the S-A-H sample, similar to that previously reported on the

surface of the S-H sample [15]. In contrast, the untreated Ti metal and the S-N-H samples exhibited flat surfaces. Figure 2(b) shows TF-XRD patterns for the Ti metal samples subjected to various treatments. The pattern for the S-H sample displayed TF-XRD peaks ascribed to Ti (PDF #44-1294), sodium titanate ($Na_2Ti_5O_{11}$) (PDF #11-0289), rutile TiO_2 (PDF #21-1276), and anatase TiO_2 (PDF #21-1272). TF-XRD peaks associated with Ti, anatase TiO_2, and rutile TiO_2 were observed in the pattern for the S-A-H sample, and those associated with Ti and rutile TiO_2 were observed in the pattern for the S-N-H sample. Figure 3 shows TF-XRD patterns for the S-A and S-N samples. The pattern for the S-A sample showed TF-XRD peaks associated with Ti, sodium hydrogen titanate ($Na_xH_{2-x}Ti_3O_7$) [28, 29], and anatase TiO_2, whereas the pattern for the S-N sample only showed peaks associated with Ti. The experimental results shown in Figs. 2(a) and 3 suggest that although the surface layer formed during NaOH treatment was completely dissolved in 1 M HNO_3 [29], it persisted even after NH_4OH treatment. In fact, it has previously been reported that sodium titanate nanowire was dissolved under acidic conditions such as in 1 M HCl [30]. Further, according to the results shown in Figs. 2(b) and 3, we can speculate that the rutile TiO_2 on the surface of the SH-NA-H sample was formed during simple thermal oxidation of Ti metal and that although a very small amount of $Na_2Ti_5O_{11}$ might be formed during subsequent heat treatment, the $Na_xH_{2-x}Ti_3O_7$ that had formed on the surface of the S-A sample was transformed into anatase and rutile TiO_2 [31].

Figure 4 shows XPS spectra containing Na_{KLL}, Ti_{2p}, O_{1s}, and N_{1s} peaks associated with samples of Ti metal subjected to various surface treatments. The Na_{KLL} XPS peak ascribed to the Na-O bond [32] was observed at around 495 eV in the spectra for the S-H and S-A-H samples; however, the intensity of the peak changed depending on the surface treatment. The peak was not observed in the spectrum for the S-N-H sample. We estimated from the areas under the Na_{KLL} XPS peaks that the concentrations of Na on the surfaces of the SH-H and S-A-H samples were 10.36 ± 1.40 and 2.93 ± 1.97 at.%, respectively. We observed that the concentration of Na remarkably decreased on the surfaces of the samples treated with either NH_4OH or HNO_3. The spectra for all samples showed Ti_{2p} XPS peaks at around 457.9 and 464.8 eV, which were ascribed to TiO_2 [33]. The spectra also showed an O_{1s} XPS peak ascribed to TiO_2 at around 529 eV [33] and a shoulder peak ascribed to OH [34] at around 530.6 eV. The concentrations of OH on the surfaces of the S-H, S-A-H, and S-N-H samples were calculated as 5.76 ± 0.61, 7.60 ± 1.02, and 9.73 ± 0.34 at.%, respectively. We observed that although the concentration of OH increased on the surfaces of the samples treated with either NH_4OH or HNO_3, the former developed apatite whereas the latter did not. Although numerous studies have previously indicated that Ti-OH

groups induced apatite nucleation [35-38], no correlation was found between the concentrations of Na and OH on the surfaces of the samples and formation of apatite in our study. The spectra for the S-H and S-A-H samples showed a single N_{1s} peak at around 399.5 eV, whereas that for the S-N-H sample showed two N_{1s} peaks at around 399.5 and 401 eV. The peak at around 399.5 eV was ascribed either to nitrogen dopant incorporated into TiO_2 as interstitial and/or impurity N atoms or to O-Ti-N, and the one at around 401 eV was ascribed to surface-adsorbed NO [39-42]. The concentrations of N on the surfaces of the S-H, S-A-H, and S-N-H samples were calculated as 0.64 ± 0.40, 0.16 ± 0.02, and 1.10 ± 0.03 at.%, respectively. Here, we note that the concentration of the impurity N on the surface of the untreated Ti plates was around 2.96 at.%. These results suggest that the impurity N partially dissolved in the NaOH and that although the concentration of N on the surface was further decreased, N-doped TiO_2 might be formed when the samples were subsequently treated with either NH_4OH or HNO_3. We cannot provide convincing explanation on the reason why the nitrogen can be entered into the surface TiO_2 by either NH_4OH or HNO_3 treatment. But, we consider that either NH_4OH or HNO_3 could be used to introduce N atoms into the surface of NaOH-treated Ti metal, because the sodium-hydrogen-titanate ($Na_xH_{2-x}Ti_3O_7$) gel layer formed during NaOH treatment of Ti metal would be highly reactive and it is reported that N-doped TiO_2 can be obtained by aqueous ammonia solution treatment of TiO_2-based materials [43].

Figures 5 show SEM photographs (a) and TF-XRD patterns (b) for samples of Ti metal subjected to various treatments and then soaked in SBF for 7 d. Apatite formed on the surfaces of the S-H and S-A-H samples; however, it did not form on the surface of the S-N-H sample. Although the extent of the formation of apatite on the surface of the S-A-H sample was slightly less than that of the formation of apatite on the surface of the S-H sample, the present results suggest that the sample of Ti metal treated with NaOH, NH_4OH, and heat has the potential to show *in vivo* bioactivity. Here, we note that although apatite did not form on the surface of the S-N-H sample, even after it was soaked in SBF for 7 d in the present study, it did form on the surface of the Ti metal sample soaked in SBF within 1 d, even after the sample was treated with NaOH, HNO_3, and heat according to the previous report [29]. The difference in the concentration of HNO_3 (present study: 1 M; previous study: 0.5–100 mM) might be responsible for the remarkable difference in the formation of apatite on the surfaces of the samples. That is, the surface structure produced when the sample was treated with NaOH might have partially remained when the sample was subsequently treated with HNO_3 in previous study, whereas the surface structure might have completely dissolved in HNO_3, as can be seen from Fig. 3, because the

concentration of HNO_3 was as high as 1 M in the present study. Table 2 summarizes crystalline phases, Na, Ti-OH, and N contents, and formation of apatite on the surfaces of samples subjected to various treatments and then soaked in SBF. According to the results shown in Table 2 and Fig. 2, the anatase TiO_2 [44, 45] and/or the fine network structure formed on the surface of the Ti metal sample treated with NaOH, NH_4OH, and heat are/is considered to be responsible for the formation of apatite on the surface of the sample soaked in SBF although the detailed mechanism for the formation of apatite is still unclear.

Figure 6 shows the decrease in the concentration of MB in samples immersed in MB solution and irradiated with visible light. The concentration of MB in the S-A-H sample decreased more than that in the untreated and S-H samples. It is interesting that S-A-H sample gave slightly better visible-light photocatalytic activity than S-H sample although the concentration of N on the surface of the S-A-H sample was smaller than that of the S-H sample (see Fig. 4 and Table 2). We speculate that the precipitation of anatase TiO_2 on sample would play some role in the expression of visible-light-induced photocatalytic activity. In fact, as can be seen in Fig. 2(b), anatase TiO_2 mainly precipitated on the surface of on the S-A-H, whereas $Na_2Ti_5O_{11}$ and rutile TiO_2 mainly precipitated with on the S-H sample. Although further detailed investigation of this phenomenon is required because not only the surface structure but also the surface area of the samples would affect the results of the evaluation of the visible-light photocatalytic activity, this preliminary result suggests that the S-A-H sample has the potential to show photocatalytic activity under visible light. Antibacterial activity test is important to directly indicate the usefulness of the S-A-H sample. However, further optimizing of condition of NaOH, NH_4OH, and heat treatments is needed prior to antibacterial activity test, because only one treatment condition was used in this study. Now we are finding the optimal treatment condition and hence we believe to report the antibacterial activity of samples in future work. In conclusion, treating the samples with NaOH, NH_4OH, and heat is useful for forming apatite on the surface of Ti metal and for producing photocatalytic activity of Ti metal under visible light. Achieving these two properties would provide novel bioactive Ti metal that exhibits antibacterial properties when subjected to visible light.

4. Conclusions

Ti metal sample treated with NaOH, NH_4OH, and heat and then soaked in SBF showed *in vitro* formation of apatite on the surface of the metal whereas that treated with NaOH, HNO_3, and heat did not. The anatase-TiO_2 precipitate and/or the fine network structure formed on the surface of the Ti metal sample treated

with NaOH, NH_4OH, and heat and soaked in SBF might be responsible for the formation of apatite on the surface of the metal. A small amount of nitrogen was on the surface of Ti metal sample treated with NaOH, NH_4OH, and heat, and the concentration of MB in that sample decreased more than in the untreated and NaOH- and heat-treated ones. The present results suggest that Ti metal treated with NaOH, NH_4OH, and heat has the potential to show bioactivity and photocatalytic activity under visible light.

Acknowledgements

This work was partially supported by a Grant-in-Aid for Challenging Exploratory Research (No. 24650271) and a Grant-in-Aid for Scientific Research (B) (No. 25282139), from the Ministry of Education, Culture, Sports, Science, and Technology, Japan. The authors thank Ms. Ohmura and Prof. Goto of the Institute for Materials Research, Tohoku University, for the XPS measurements and data analysis.

References

[1] G.E. Hill and D.G. Droller, Orthop. Rev., 18 (1989) 617.

[2] A.B. Wymenga, J.R. van Horn, A. Theeuwes, H.L. Muytjens and T. J. Slooff, Acta Orthop. Scand., 63 (1992) 665.

[3] C.B. Phillips, J.A. Barrett, E. Losina, N.N. Mahomed, E.A. Lingard, E. Guadagnoli, J.A. Baron, W.H. Harris, R. Poss and J.N. Katz, J. Bone Joint Surg. Am., 85-A (2003) 20.

[4] S. Bengtson and K. Knutson, Acta Orthop. Scand., 62 (1991) 301.

[5] R.S. Petrie, A.D. Hanssen, D.R. Osmon and D. Ilstrup, Am. J. Orthop., 27 (1998) 172.

[6] G. Magyar, S. Toksvig-Larsen and A. Lindstrand, J. Bone Joint Surg. Br., 81 (1999) 449.

[7] M. Bosetti, A. Masse, E. Tobin and M. Cannas, Biomaterials, 23 (2002) 887.

[8] G. Gosheger, J. Hardes, H. Ahrens, A. Streitburger, H. Buerger, M. Erren, A. Gunsel, F.H. Kemper, W. Winkelmann and C. von Eiff, Biomaterials, 25 (2004) 5547.

[9] W. Chen, Y. Liu, H.S. Courtney, M. Bettenga, C.M. Agrawal, J.D. Bumgardner and J.L. Ong, Biomaterials, 27 (2006) 5512.

[10] I. Noda, F. Miyaji, Y. Ando, H. Miyamoto, T. Shimazaki, Y. Yonekura, M. Miyazaki, M. Mawatari and T. Hotokebuchi, J. Biomed. Mater. Res. Part B: Appl. Biomater., 89B (2009) 456.

[11] C.N. Kraft, M. Hansis, S. Arens, M.D. Menger and B. Vollmar, J. Biomed. Mat. Res., 49 (2000) 192.

[12] A. Masse, A. Bruno, M. Bosetti, A. Biasibetti, M. Cannas and P. Gallinaro, J. Biomed. Mater. Res., 53 (2000) 600.

[13] T. Shirai, T. Shimizu, K. Ohtani, Y. Zen, M. Takaya and H. Tsuchiya, Acta Biomater., 7 (2011) 1928.

[14] H. Tsuchiya, T. Shirai, H. Nishida, H. Murakami, T. Kabata, N. Yamamoto, K. Watanabe and J. Nakase, J. Orthop. Sci., 17 (2012) 595.

[15] H.-M. Kim, F. Miyaji, T. Kokubo and T. Nakamura, J. Biomed. Mater. Res., 32 (1996) 409.

[16] W.-Q. Yan, T. Nakamura, M. Kobayashi, H.-M. Kim, F. Miyaji and T. Kokubo, J. Biomed. Mater. Res., 37 (1997) 267.

[17] T. Kokubo, H. Takadama and M. Matsushita, in T. Kokubo (Ed.), Bioceramics and Their Clinical Applications, Woodhead Pub. Ltd., Cambridge, 2008, Chapter 21.

[18] T. Kizuki, T. Matsushita and T. Kokubo, in M. Niinomi (Eds.), Development of Antibacterial Bioactive Ti Metal and its Alloy, Proc. 2012 Symposium Japanese Society for Biomaterials, Sendai, November 27, Japanese Society for Biomaterials Symposium 2012, Sendai, 2012, p. 250.

[19] B.C. Yang, M. Uchida, H.-M. Kim, X.D. Zhang and T. Kokubo, Biomaterials, 25 (2004) 1003.

[20] X. Cui, H.-M. Kim, M. Kawashita, L. Wang, T. Xiong, T. Kokubo and T. Nakamura, Dent. Mater., 25 (2009) 80.

[21] B. Liang, S. Fujibayashi, M. Neo, J. Tamura, H.-M. Kim, M. Uchida, T. Kokubo and T. Nakamura, Biomaterials, 24 (2003) 4959.

[22] S. Sato, Chem. Phys. Lett., 123 (1986) 126.

[23] R. Asahi, T. Morikawa, T. Ohwaki, K. Aoki and Y. Taga, Science, 293 (2001) 269.

[24] R. Bacsa, J. Kiwi, T. Ohno, P. Albers and V. Nadtochenko, J. Phys. Chem. B, 109 (2005) 5994.

[25] S.B. Cho, K. Nakanishi, T. Kokubo, N. Soga, C. Ohtsuki, T. Nakamura, T. Kitsugi and T. Yamamuro, J. Am. Ceram. Soc., 78 (1995) 1769.

[26] T. Kokubo and H. Takadama, Biomaterials, 27 (2006) 2907.

[27] M. Kamitakahara, O. Kawaguchi, N. Watanabe and K. Ioku, Mater. Res. Bull., 46 (2011) 2283.

[28] X. Sun and Y. Li, Chem. Eur. J., 9 (2003) 2229.

[29] D.K. Pattanayak, S. Yamaguchi, T. Matsushita and T. Kokubo, J. Mater. Sci.: Mater. Med., 22 (2011) 1803.

[30] B. Schürer, M.J. Elser, A. Sternig, W. Peukert and O. Diwald, J. Phys. Chem. C, 115 (2011) 12381.

[31] S. Papp, L. Kõrösi, V. Meynen, P. Cool, E.F. Vansant and I. Dékány, J. Solid State Chem., 178 (2005) 1614.

[32] A. Barrie and F.J. Street, J. Electron. Spectrosc. Relat. Phenom., 7 (1975) 1.

[33] F.A. Akin, H. Zreiqat, S. Jordan, M.B.J. Wijesundara and L. Hanley, J. Biomed. Mater. Res., 57 (2001) 588.

[34] Y. Nakao, A. Sugino, K. Tsuru, K. Uetsuki, Y. Shirosaki, S. Hayakawa and A. Osaka, J. Ceram. Soc. Jpn., 118 (2010) 483.

[35] P. Li, C. Ohtsuki, T. Kokubo, K. Nakanishi, N. Soga, T. Nakamura, T. Yamamuro and K. de Groot, J. Biomed. Mater. Res., 28 (1994) 7.

[36] T. Kasuga, H. Kondo and M. Nogami, J. Cryst. Growth, 235 (2002) 235.

[37] T. Kokubo, H.-M. Kim and M. Kawashita, Biomaterials, 24 (2003) 2161.

[38] H. Maeda, T. Kasuga and M. Nogami, J. Eur. Ceram. Soc., 24 (2004) 2125.

[39] X. Chen, Y.-B. Lou, A.C.S. Samia, C. Burda and J.L. Gole, Adv. Func. Mater., 15 (2005) 41.

[40] M. Sathish, B. Viswanathan, R.P. Viswanath and C.S. Gopinath, Chem. Mater., 17 (2005) 6349.

[41] G. Liu, H.G. Yang, X. Wang, L. Cheng, J. Pan, G.Q. Lu and H.-M. Cheng, J. Am. Chem. Soc., 131 (2009) 12868.

[42] J. Zhang, J. Xi and Z. Ji, J. Mater. Chem., 22 (2012) 17700.

[43] T. Matsumoto, N. Iyi, Y. Kaneko, K. Kitamura, Y. Takasu and Y. Murakami, Chem. Lett., 5 (2004) 1508.

[44] T. Kawai, T. Kizuki, H. Takadama, T. Matsushita, H. Unuma, T. Nakamura and T. Kokubo, J. Ceram. Soc. Jpn., 118 (2010) 19.

[45] M. Kawashita, N. Matsui, T. Miyazaki and H. Kanetaka, Mater. Trans., 54 (2013) 811.

Figure legends

Figure 1 Schematic illustration of apparatus used to evaluate visible-light photocatalytic activity.

Figure 2 SEM photographs (a) and TF-XRD patterns (b) of Ti metal subjected to various surface treatments.

Figure 3 TF-XRD patterns for samples SH-AS and SH-NA.

Figure4 XPS spectra containing Na_{KLL}, Ti_{2p}, O_{1s}, and N_{1s} peaks for Ti metal subjected to various surface treatments.

Figure 5 SEM photographs (a) and TF-XRD patterns (b) of Ti metal subjected to various surface treatments and then soaked in SBF for 7 d.

Figure 6 Decrease in concentration of MB due to irradiating immersed samples with visible light (mean ± SD, n=5).

Table legends

Table 1 Abbreviated names of samples subjected to various surface treatments.

Table 2 Crystalline phases, Na, Ti-OH, and N contents (mean ± SD, n=5), and formation of apatite on surfaces of samples subjected to various surface treatments and then soaked in SBF.

Figure(s)

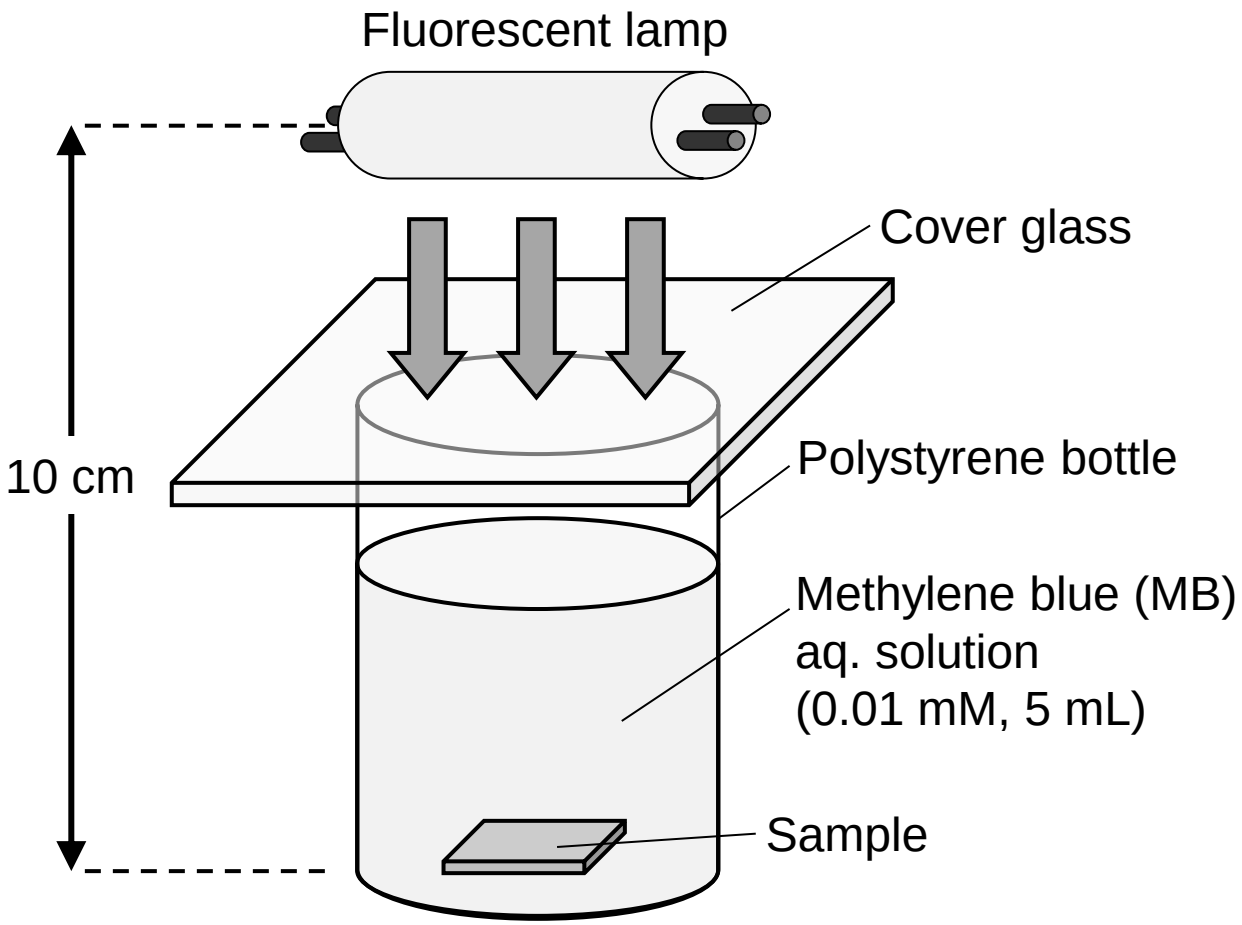

Figure 1 Kawashita *et al.*

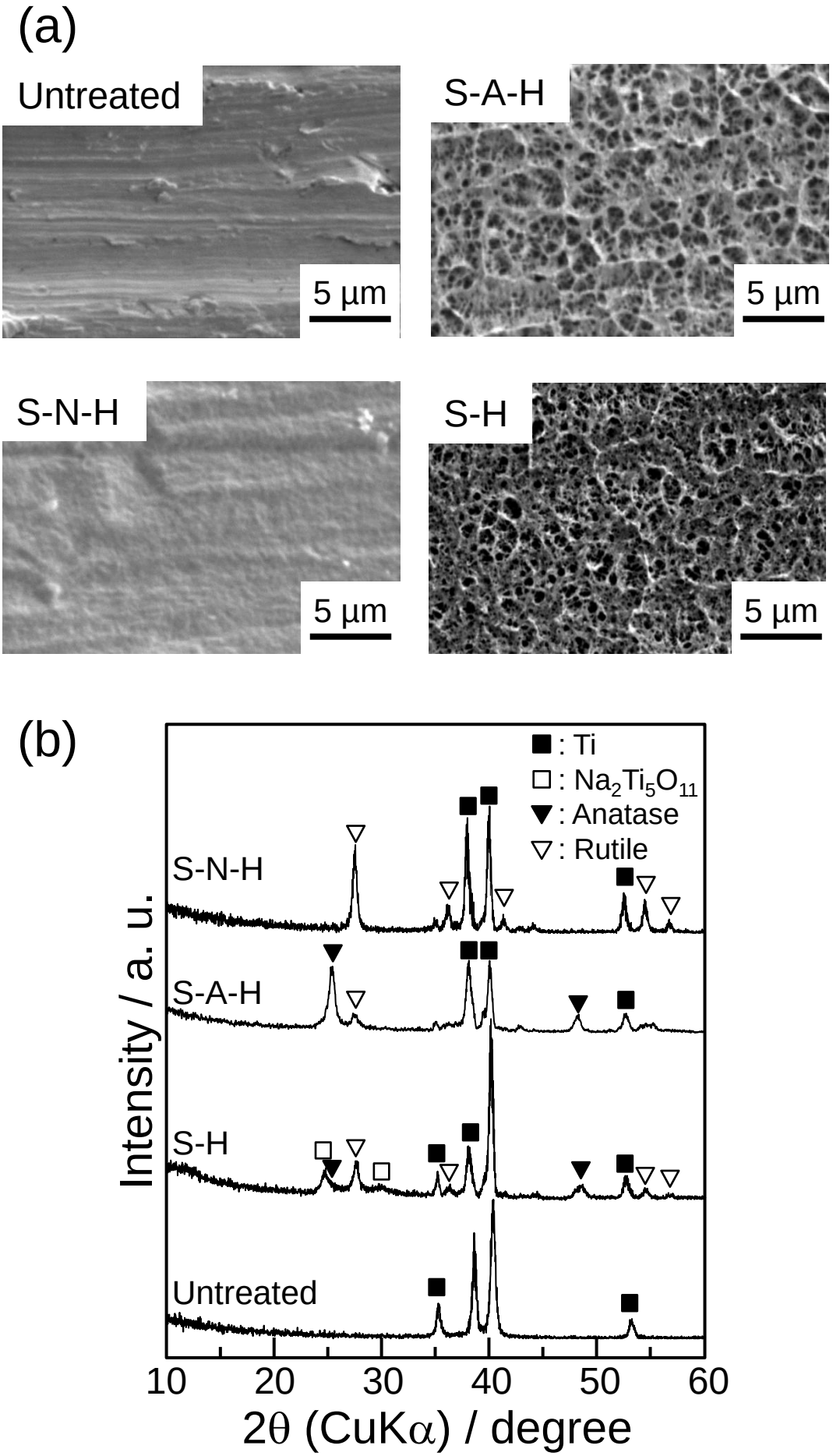

Figure 2 Kawashita *et al.*

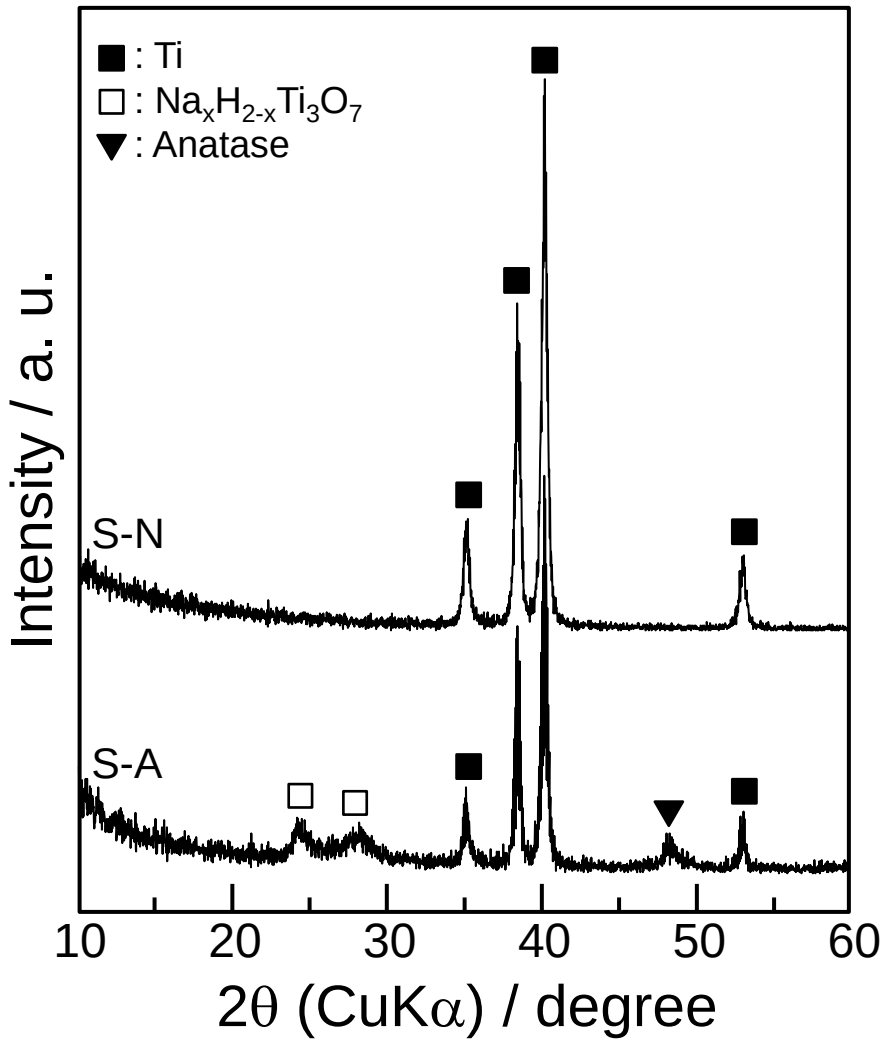

Figure 3 Kawashita *et al.*

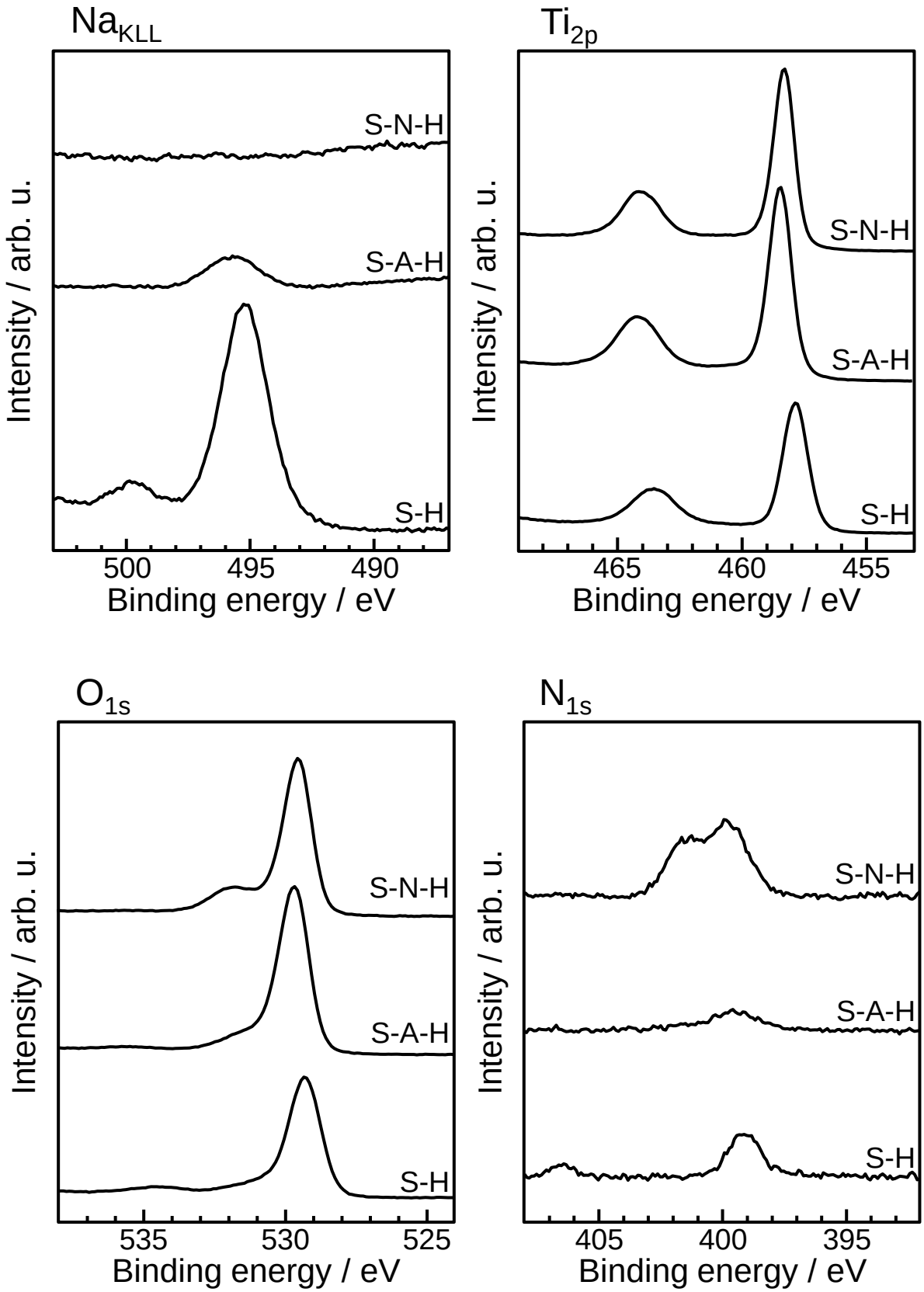

Figure 4 Kawashita *et al.*

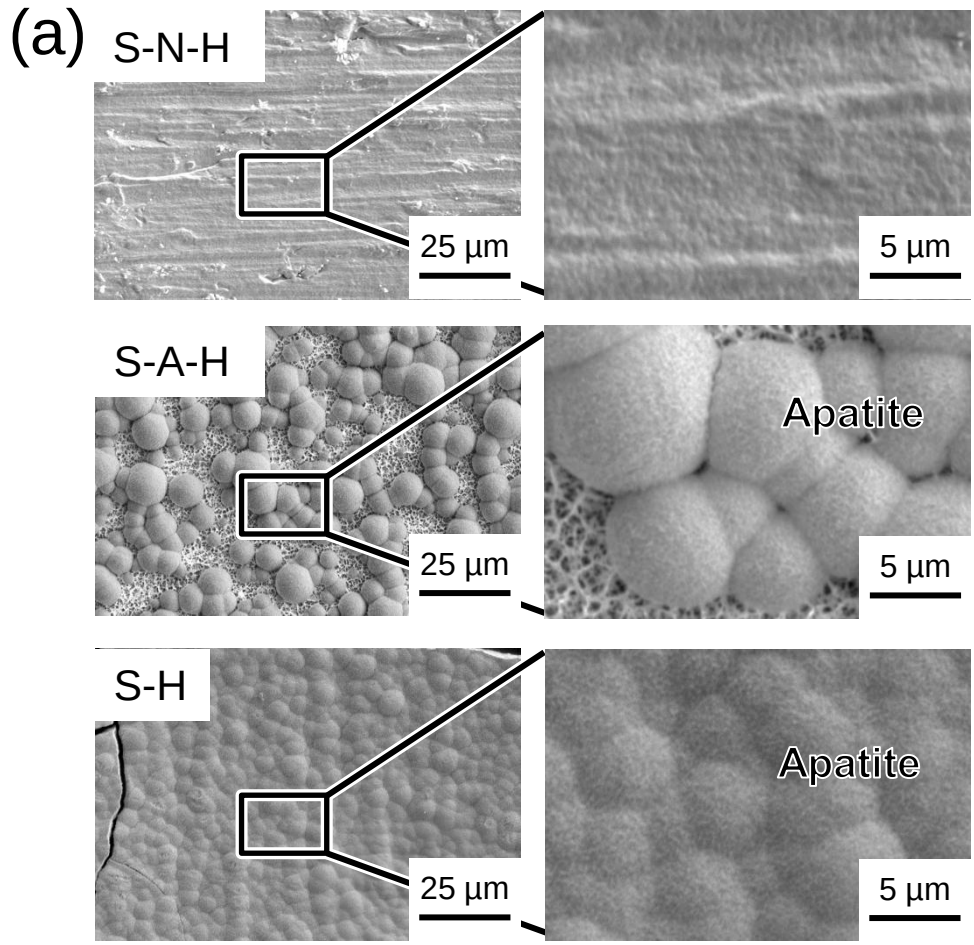

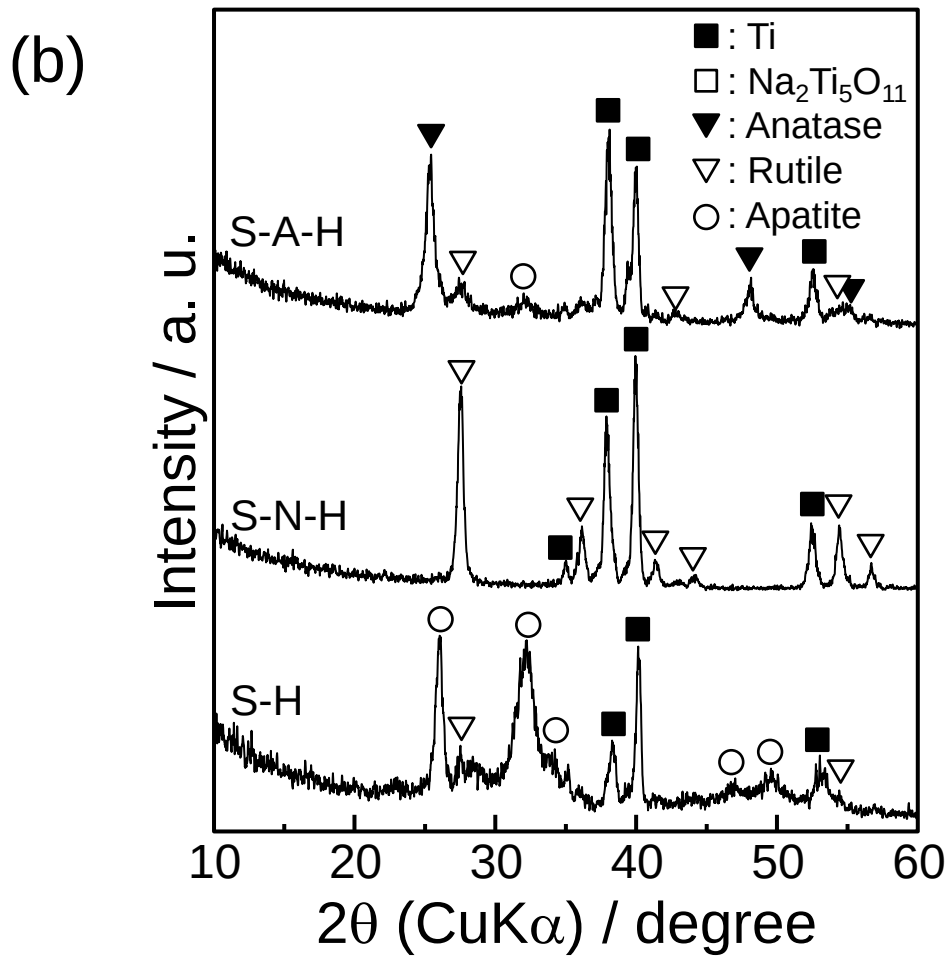

Figure 5 Kawashita *et al.*

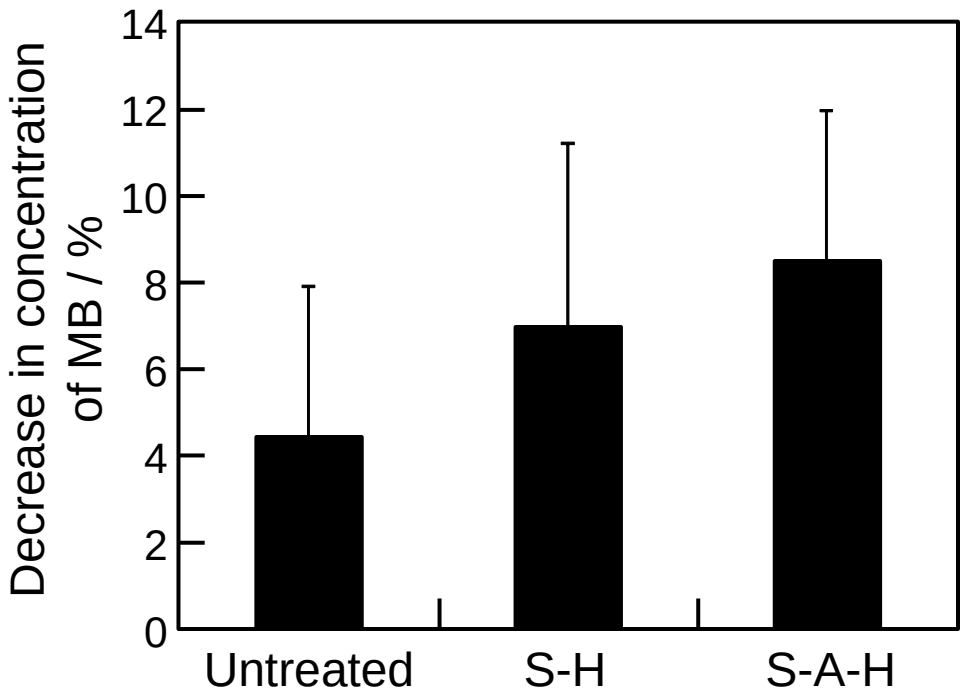

Figure 6 Kawashita *et al.*

Treatments	Abbreviated name
NaOH + heat	S-H
NaOH + NH_4OH	S-A
NaOH + NH_4OH + heat	S-A-H
NaOH + HNO_3	S-N
NaOH + HNO_3 + heat	S-N-H

Table 1 Kawashita *et al.*

Sample	Crystalline phase	Na content / at.%	Ti-OH content / at.%	N content / at.%	Apatite formation in SBF
S-N-H	Ti, R	0.04 ± 0.02	9.73 ± 0.34	1.10 ± 0.03	No
S-A-H	Ti, A, R	2.93 ± 1.97	7.60 ± 1.02	0.16 ± 0.02	Yes
S-H	Ti, ST, A, R	10.36 ± 1.40	5.76 ± 0.61	0.64 ± 0.40	Yes

Table 2 Kawashita *et al.*